Table 1. y_2 *and* y_3 *as functions of* x_s

x_s	y_2	y_3	x_s	y_2	y_3
0	1	0	3	0·2938	0·0806
0·05	0·9521	0·0079	4	0·2526	0·0794
0·1	0·9086	0·0150	5	0·2246	0·0776
0·2	0·8323	0·0269	6	0·2040	0·0758
0·3	0·7680	0·0366	7	0·1882	0·0740
0·4	0·7133	0·0445	8	0·1755	0·0723
0·5	0·6664	0·0509	9	0·1650	0·0707
0·6	0·6258	0·0561	10	0·1562	0·0692
0·7	0·5906	0·0604	20	0·1091	0·0588
0·8	0·5598	0·0640	30	0·0887	0·0526
0·9	0·5325	0·0670	40	0·0766	0·0484
1	0·5084	0·0694	50	0·0684	0·0452
2	0·3628	0·0797			

These expressions can also be written as

$$y_0 = y^\infty = \frac{1}{2x_s}\int_0^{2x_s} e^{-u} I_0(u)\,du$$

$$y_1 = \frac{1}{2x_s}\int_0^{2x_s} du \int_0^{u} e^{-v} I_0(v)\,dv.$$

From Appendix *B* and the identity,

$$I_2(x) = I_0(x) - \frac{2}{x} I_1(x),$$

$$y_0 = y^\infty = e^{-2x_s}[I_0(2x_s) + I_1(2x_s)] \qquad (C.6)$$

$$y_1 = \frac{4}{3} y_0 - \frac{1}{3x_s} e^{-2x_s} I_1(2x_s). \qquad (C.7)$$

Finally, let the ${}_qF_q$ generalized hypergeometric series be

$${}_pF_q(a_1, \ldots, a_p; b_1, \ldots, b_q; z) = \sum_{n=1}^{\infty} \frac{(a_1)_n \ldots (a_p)_n}{(b_1)_n \ldots (b_q)_n} \frac{z^n}{n!} \qquad (C.8)$$

with $(a)_n = \Gamma(a+n)/\Gamma(a)$.

Then, it follows that

$$y_2 = 1 + {}_2F_2[\tfrac{1}{2}, \tfrac{3}{2}; 1, 3; -4x_s]$$
$$y_3 = \frac{x_s}{6}\{1 + {}_2F_2[\tfrac{3}{2}, \tfrac{3}{2}; 2, 4; -4x_s]\}. \qquad (C.9)$$

y_2 and y_3 are given as functions of x_s in Table 1.

References

ABRAMOWITZ, M. & STEGUN, A. (1965). *Handbook of Mathematical Functions.* New York: Dover.

BECKER, P. (1977). *Acta Cryst.* A**33**, 667–671.

BECKER, P. & COPPENS, P. (1974). *Acta Cryst.* A**30**, 129–147.

BONNET, M., DELAPALME, A., BECKER, P. & FUESS, H. (1976). *Acta Cryst.* A**32**, 945–953.

DUNSTETTER, F. (1981). Thèse de 3ème cycle, Paris.

KATO, N. (1976). *Acta Cryst.* A**32**, 453–466.

KATO, N. (1979). *Acta Cryst.* A**35**, 9–16.

KATO, N. (1980*a*). *Acta Cryst.* A**36**, 171–177.

KATO, N. (1980*b*). *Acta Cryst.* A**36**, 763–778.

KATO, N. (1980*c*). In *Electron and Magnetization Densities in Molecules and Crystals*, edited by P. BECKER. New York: Plenum.

KATO, N. (1982). Sagamore VII Conference Abstracts.

SAKA, T., KATAGAWA, T. & KATO, N. (1972). *Acta Cryst.* A**29**, 192–200.

Acta Cryst. (1984). A**40**, 251–254

Resolution Revisited: Limit of Detail in Electron Density Maps

BY RONALD E. STENKAMP AND LYLE H. JENSEN

Department of Biological Structure and Department of Biochemistry, University of Washington, School of Medicine, Seattle, WA 98195, *USA*

(*Received* 2 *September* 1983; *accepted* 7 *November* 1983)

Abstract

Application of the Rayleigh criterion for the limit of resolution of a simple lens with axial illumination leads to the value 0·61λ. In two-dimensional electron density maps based on X-ray data, the limit of resolution has been considered to be 0·61 d_{min}, the counterpart of the optical case, and in three-dimensional maps 0·715 d_{min}. It is shown here that point atoms separated by these distances are not resolved in two- and three-dimensional electron density maps. Such maps are amplitude functions rather than intensity functions as in the optical case. Application of the Rayleigh criterion to the three-dimensional amplitude function for point atoms leads to a value of 0·917 d_{min} for the limit of resolution in three-dimensional electron density maps. This result is confirmed by superposing both analytic and numeric functions for point atoms and numeric functions for real atoms with $B = 0$ and 10 Å^2. Finally, some implications of diffraction effects in X-ray structure analysis are considered.

In refining models for the met and azidomet forms of hemerythrin, we were particularly interested in the

0108-7673/84/030251-04$01.50

bond lengths and angles in the binuclear iron complexes present in these proteins (Stenkamp, Sieker & Jensen, 1982, 1983). The structures are relatively large (Stenkamp & Jensen, 1979), and we were concerned about the accuracy of the atomic parameters in the complexes because the Fe–X bond lengths are near the 2 Å minimum interplanar distances (d_{min}) of the present data sets. In considering the possible effects of diffraction ripples from the Fe atoms on the positions of the ligand atoms, we restudied the matter of resolution in electron density maps and were led to an unexpected result.

The optical case

It has long been known that the limit of detail that can be resolved by an optical system is ultimately determined by the wavelength of the radiation (Sommerfeld, 1954). Application of the Rayleigh criterion (Sommerfeld, 1954; Strong, 1958) for resolution in the theory of diffraction-limited image formation leads to the equation

$$\text{limit} = 0{\cdot}61\lambda \qquad (1)$$

for the minimum separation of structures that can be imaged separately by a circular lens with a numerical aperture of unity and axial illumination (Sommerfeld, 1954).

The pattern of diffraction rings surrounding the image of a very small circular aperture is well known (Strong, 1958). A trace through the center of such an image is shown in Fig. 1(*a*). For the maxima in the image of two such apertures to be resolved, the Rayleigh criterion holds that the maximum of one be superposed on the first minimum of the other. Fig. 1(*b*) shows a trace through two images separated according to the Rayleigh criterion. The distance of the first minimum from the central maximum is the nominal limit of resolution expressed by (1) (Sommerfeld, 1954; Strong, 1958).

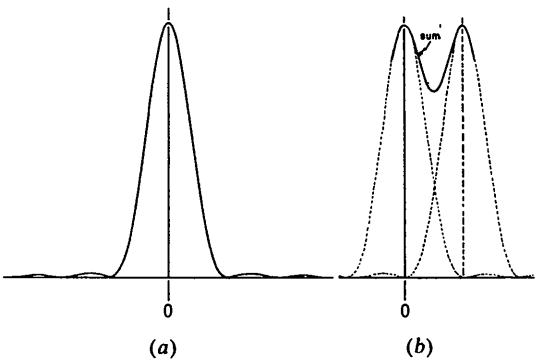

Fig. 1. (*a*) Optical diffraction from a very small circular aperture. (*b*) Optical diffraction from two very small circular apertures separated according to the Rayleigh criterion (0·61λ).

The X-ray case

James (1948, 1965) has treated resolution in terms of false detail in Fourier maps based on X-ray data. He assumes scattering from point atoms at rest in one-, two- and three-dimensional lattices.

In the two-dimensional case, the counterpart of image formation by a lens, James derived a general equation (equation 12, James, 1948) expressing the electron density ρ as a function of d_{min} of the data, $F(0)$, the constant value of the structure factors, and r, the radial distance from the atomic center. To illustrate diffraction ripples and resolution for a particular case, we choose $d_{min} = 2$ Å. For this case, the general equation reduces to the following:

$$\rho(r)_{2D} = (1/2)F(0)J_1(\pi r)/\pi r, \qquad (2)$$

where J_1 is the first-order Bessel function. We plot $\rho(r)_{2D}$ *vs* r as curve II in Fig. 2, normalized to unity at $r = 0$. In contrast to the optical case in Fig. 1(*a*) where *intensities* are plotted and the function is nowhere negative, curve II is alternatively positive and negative because it represents an *amplitude* function. Although curve II is for the special case of data with $d_{min} = 2$ Å, the phenomenon displayed is general, and the same pattern of ripples, except for the horizontal scale, occurs for any finite d_{min}.

In considering detail that can be resolved in two-dimensional electron density maps, James (1965) took the *radius* of the central maximum, *i.e.* the value of r at the first zero of the function represented by curve

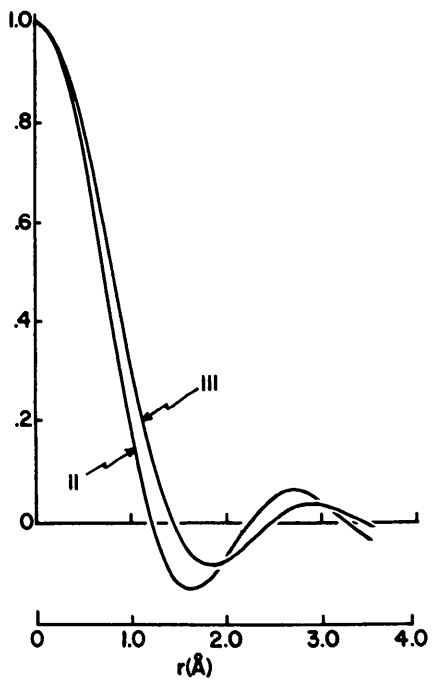

Fig. 2. Relative electron density, $\rho(r)$, for point atoms as a function of r for X-ray data with $d_{min} = 2$ Å. II, the two-dimensional function: III, the three-dimensional function.

II, as the limit of resolution. From (2), this occurs at $r = 1{\cdot}22$ Å for data with $d_{min} = 2$ Å, or, in terms of d_{min},

$$\text{limit} = 0{\cdot}61\ d_{min}. \quad (3)$$

Equation (3) for the two-dimensional X-ray case corresponds to (1) for the optical case. The similarity follows from the fact that the first zero of the amplitude function in terms of d_{min} is the same as the first minimum of the intensity function in terms of λ.

We now ask whether point atoms separated by 1·22 Å in projection can be resolved in an electron density map based on data with $d_{min} = 2$ Å. Fig. 3 shows the result of superposing two $\rho(r)_{2D}$ functions separated by 1·22 Å. Clearly, the maxima of the two functions are not resolved in the sum: they merge and appear as a single peak.

In the three-dimensional X-ray case, James derived a general equation (equation 7, James, 1948) which reduces to the following for data with $d_{min} = 2$ Å:

$$\rho(r)_{3D} = (\pi/2)F(0)[(\sin \pi r - \pi r \cos \pi r)/\pi^3 r^3], \quad (4)$$

the symbols carrying the same meaning as before. The function normalized to unity at $r = 0$ is plotted as curve III in Fig. 2. The radius of the central maximum of the function, again based on data with $d_{min} = 2$ Å, is 1·43 Å, or, in terms of d_{min},

$$r = 0{\cdot}715\ d_{min} \quad (5)$$

(James, 1948). Although James does not state that (5) represents the limit of resolution for three-dimensional X-ray data, it is, nevertheless, the counterpart of (3) for the two-dimensional case and is generally regarded as expressing the limit of resolution that can be achieved in three-dimensional electron density maps (Blundell & Johnson, 1976).

We have tested for resolution according to (5) by superposing two functions represented by curve III, separated by a distance of 1·43 Å = 0·715 d_{min}, Fig. 4(*a*). The result is similar to the two-dimensional case: the peaks are not resolved in the sum; only a single maximum results.

In seeking an alternative to (5), we have applied the Rayleigh criterion to the three-dimensional amplitude function, taking the value of r at the *first minimum* of the function as the nominal limit of resolution. Since the first minimum of curve III based on data with $d_{min} = 2$ Å occurs at 1·834 Å, the proposed limit of resolution in terms of d_{min} becomes

$$\text{limit} = 0{\cdot}917\ d_{min}. \quad (6)$$

Fig. 4(*b*) shows the result of testing for resolution according to (6). The atoms are obviously resolved, the value midway between the maxima being 0·834 of its value at the peak positions.

We have checked the results shown in Figs. 4(*a*), (*b*) by a numerical calculation, assuming two point nitrogen atoms separated by distances of 1·43 and 1·83 Å in primitive triclinic lattices, calculating the structure factors and truncating the data sets at d_{min} = 2 Å. Plots of $\rho(r)_{3D}$ on the lines joining the two pairs of atoms are shown in Figs. 5(*a*), (*b*). Point atoms separated by 1·43 Å are not resolved but, when they are separated by 1·83 Å, resolution is clearly achieved. The plots in Figs. 5(*a*), (*b*) based on calculated structure factors are, when properly scaled, virtually identical to the sum functions in Figs. 4(*a*), (*b*) based on James's (1948) equation.

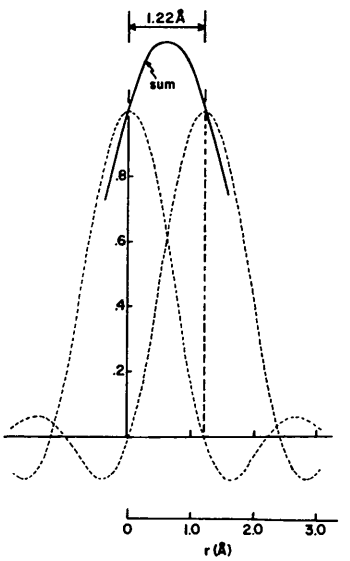

Fig. 3. Composite $\rho(r)_{2D}$ (——) for two point atoms separated by 1·22 Å = 0·61 d_{min} for X-ray data with $d_{min} = 2$ Å.

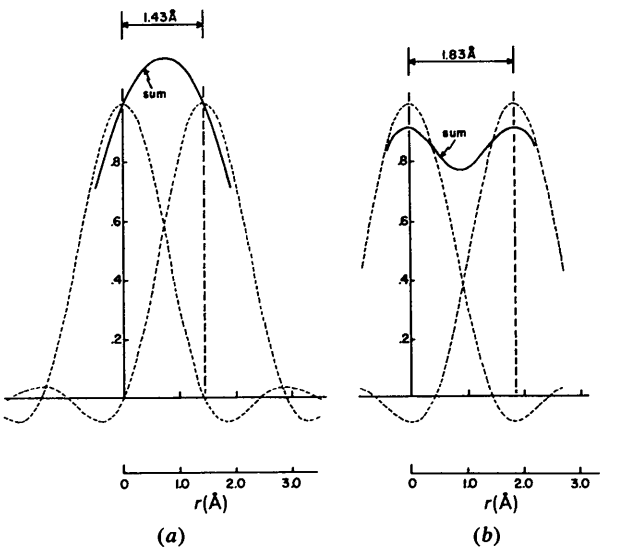

Fig. 4. (*a*) Composite $\rho(r)_{3D}$ (——) for two point atoms separated by 1·43 Å = 0·715 d_{min} for X-ray data with $d_{min} = 2$ Å. (*b*) Composite $\rho(r)_{3D}$ (——) for two point atoms separated by 1·834 Å = 0·917 d_{min} for X-ray data with $d_{min} = 2$ Å.

Some implications

In practice we do not expect to achieve the resolution in electron density maps indicated by (6), because atoms are not point scatterers. To determine the effects of atomic size and thermal motion on resolution, we repeat the numerical calculations of the preceding paragraph, first for nitrogen atoms at rest, Fig. 6(*a*) (scattering factors from *International Tables for X-ray Crystallography*, 1962), and then for nitrogen atoms with isotropic B values corresponding to 10 Å^2, Fig. 6(*b*). The atoms are resolved in both instances, although less well resolved as the spread in electron density increases and the peak height decreases.

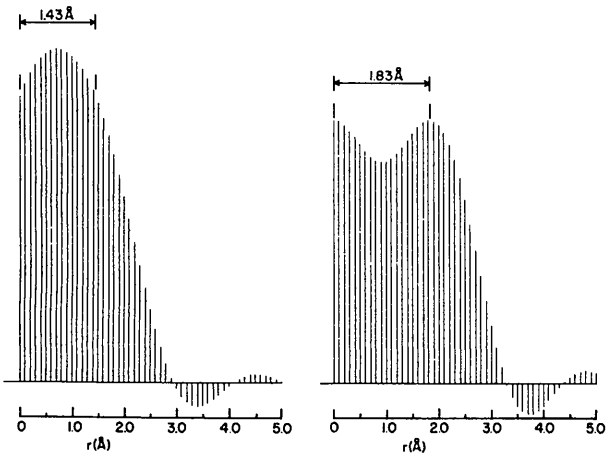

Fig. 5. (*a*) Numerical calculation of composite $\rho(r)_{3D}$ for two point N atoms separated by 1·43 Å = 0·715 d_{min} for X-ray data truncated at d_{min} = 2 Å. (*b*) Numerical calculation of composite $\rho(r)_{3D}$ for two point N atoms separated by 1·834 Å = 0·917 d_{min} for X-ray data truncated at d_{min} = 2 Å.

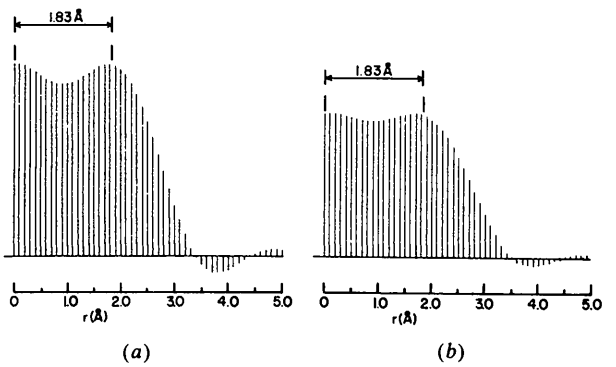

Fig. 6. (*a*) Numerical calculation of composite $\rho(r)_{3D}$ for two N atoms, typical form factors and B = 0 Å^2, separated by 1·834 Å = 0·917 d_{min} for X-ray data truncated at d_{min} = 2 Å. (*b*) Numerical calculation of composite $\rho(r)_{3D}$ for two N atoms, typical form factors and B = 10 Å^2, separated by 1·834 Å = 0·917 d_{min} for X-ray data truncated at d_{min} = 2 Å.

The effect of atomic size on resolution is evident by comparing Fig. 5(*b*) for point nitrogen atoms with Fig. 6(*a*) for nitrogen atoms at rest. The additional effect of thermal motion corresponding to B = 10 Å is seen by comparing Figs. 6(*a*) and (*b*). Clearly, resolution is impaired at higher B values, and at some $B > 10$ Å^2 nitrogen atoms separated by 1·83 Å will not be resolved by data limited at d_{min} = 2 Å.

The numeric results plotted in Figs. 6(*a*), (*b*) are based on perfect data and represent the best that can be achieved in resolution under the assumed conditions. In electron density maps based on experimental data, errors in the observed amplitudes and derived phases will impair the resolution. Therefore, the practice common among macromolecular crystallographers of quoting the limit of resolution as d_{min} is fully justified.

The diffraction ripples in electron density maps represent termination of series error resulting from the finite series used in calculating $\rho(x, y, z)$. Not only do these ripples limit resolution, as we have seen, but they also affect the positions of the atoms in electron density maps. Although such maps are no longer of central importance in refining molecular models based on X-ray data, other refinement techniques such as least squares may share the effects in subtle, less obvious ways (Cochran, 1948; Cruickshank, 1952; see also Booth, 1946; Cochran, 1951).

This work has been supported by USPHS Grant GM-10828 from the National Institutes of Health and equipment grant PCM 76-20557 from the National Science Foundation.

References

BLUNDELL, T. L. & JOHNSON, L. N. (1976). *Protein Crystallography*, pp. 117, 381. New York: Academic Press.

BOOTH, A. D. (1946). *Proc. R. Soc. London, Ser. A*, **188**, 77–92.

COCHRAN, W. (1948). *Acta Cryst.* **1**, 138–142.

COCHRAN, W. (1951). *Acta Cryst.* **4**, 408–411.

CRUICKSHANK, D. W. J. (1952). *Acta Cryst.* **5**, 511–518.

International Tables for X-ray Crystallography (1962). Vol. III, pp. 202–203. Birmingham: Kynoch Press.

JAMES, R. W. (1948). *Acta Cryst.* **1**, 132–134.

JAMES, R. W. (1965). *The Crystalline State.* Vol. II. *The Optical Principles of the Diffraction of X-rays*, pp. 385–403. Ithaca: Cornell Univ. Press.

SOMMERFELD, A. (1954). *Optics*, pp. 225–227, 289, 306–309. New York: Academic Press.

STENKAMP, R. E. & JENSEN, L. H. (1979). In *Advances in Inorganic Biochemistry*, Vol. 1, pp. 219–233, edited by G. L. EICHHORN & L. G. MARZILLI. Amsterdam: Elsevier/North Holland.

STENKAMP, R. E., SIEKER, L. C. & JENSEN, L. H. (1982). *Acta Cryst.* B**38**, 784–792.

STENKAMP, R. E., SIEKER, L. C. & JENSEN, L. H. (1983). *Acta Cryst.* B**39**, 697–703.

STRONG, J. (1958). *Concepts of Classical Optics*, pp. 203–207, 210–212. San Francisco: W. H. Freeman.